Research Paper

Isolation of Lysozyme from Chicken Egg White by Surface Charged Membranes

Nandala Shiva Prasad [1, 2, 3], Aarti Tallam [1], Namita Roy Choudhury [3], Sundergopal Sridhar [1, 2, *], Suresh K. Bhargava [3]

[1] Membrane Separations Laboratory, Process Engineering and Technology Transfer Division, CSIR - Indian Institute of Chemical Technology, Hyderabad, India-500007.
[2] Academy of Scientific and Innovative Research (AcSIR), Ghaziabad, Uttar Pradesh, India.
[3] Royal Melbourne Institute of Technology (RMIT), Melbourne, VIC 3001, Australia.

Article info

Keywords

Highlights

- Negatively charged membranes were fabricated using sulfonated PES.
- Permeation flux was enhanced under cross-flow over dead-end filtration.
- sPES membranes exhibited a low fouling tendency for protein adsorption.
- Semi-batch protein isolation demonstrated selective separation of Lysozyme.

Graphical abstract
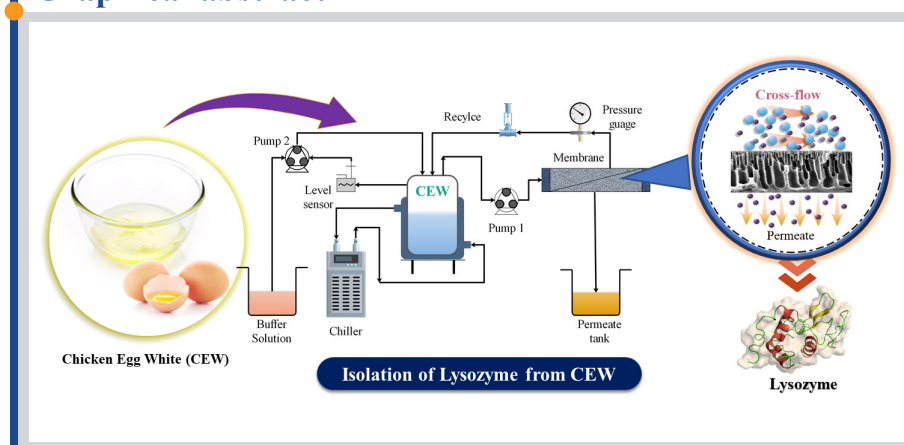
Abstract

The fabrication of innovative and resourceful ultrafiltration membranes for the separation of protein mixtures is significantly required, principally in the food and pharmaceutical manufacturing sectors. The current research focuses on the preparation of surface-charged membranes by polyethersulfone (PES)/ sulfonated polyethersulfone (sPES) membranes blended with different molecular weight cut-off (MWCO) polyethylene glycol (PEG) for the separation of Lysozyme from natural chicken egg white (CEW). The synthesized membranes were characterized by scanning electron microscopy (SEM), atomic force microscopy (AFM), contact angle, and porosity. By examining the morphological changes and the effect of physicochemical parameters, the optimized process condition to attain maximum lysozyme separation was determined. In the semi-batch mode of operation, the sPES-PEG400 membrane exhibited maximum Lysozyme transmission and high fouling resistance. The outcomes of the present study led to an in-depth understanding of the interrelationship between the PES/sPES with PEG, which sheds light on the use of membrane technology in complex protein mixture separation.

1. Introduction

Downstream processing and isolation of proteins have gained tremendous attention in the last two decades due to their vast industrial applications, especially in the pharmaceutical [1-3] and food industries [4-6]. Purification of proteins involves intensive separation techniques such as electrophoresis [7,8], packed bed column chromatography [9], and ion exchange chromatography [10-12]. On the other hand, the techniques used in the laboratory procedures for protein purification are proficient in processing small quantities. However, laboratory processes are complicated to scale up as they involve complex instrumentation to yield high-purity proteins. Indeed, packed bed column chromatography is widely practiced commercially for large-scale protein separation, where the operational and regeneration costs are the primary concern due to slow mass transfer, high process pressure drops, and lengthy operational procedures [5,13]. Therefore, the rapid expansion in the biotechnology, pharmaceutical, and food industry demands a cost-effective large-scale protein purification technique.

Lysozyme is one of the most widely consumed proteins in food and pharmaceutical applications as a preservative agent [5,14], anti-microbial [1,15], anti-inflammatory [4,16], anticancer drug [2,3,17-19], respectively.

Additionally, lysozyme acts as an antibacterial protein, which can cleave the peptidoglycan layer of the bacteria cell wall by disrupting ß-linkages between the N-acetyl-D-glucosamine and N-acetylmuramic acid [5,20]. Furthermore, Lysozyme has potential applications in human cancer chemotherapy in addition to the anticancer drug [21,22].

Traditionally, Lysozyme is extracted from chicken egg white (CEW) by hybrid processes combining crystallization, precipitation, chromatography, and adsorption [23]. Nevertheless, these methods are generally tedious, complicated, and costly for large-scale production of Lysozyme. Besides the low concentration of Lysozyme in crude CEW became a crucial challenge in the development of separation techniques since large volumes of process streams need to be handled to produce a reasonable amount of pure Lysozyme [21]. In recent times, various innovative techniques have been proposed [5,24-29], in which the membrane separation process is one of the emerging technologies. Ultrafiltration being a powerful tool for bio-separation, the significant advantage is that proteins can be easily separated based on the size exclusion principle and are free from foreign particles. Ghosh and Cui have used the commercial polysulfone membranes of 25 and 50 kDa MWCO and studied the effect of different functional parameters (pH, pressure, system hydrodynamics) for the separation of Lysozyme from CEW. High purity of Lysozyme of 98.7% was achieved through a 25 kDa membrane at a transmembrane pressure of 80 kPa and pH of 11 [30]. In addition, the variation of purity levels of Lysozyme with the pre-treatment of 50 kDa polysulfone membrane using myoglobin was also discussed. The separation of Lysozyme was 26% superior by using a pre-treated membrane with a purity of 96% at 120 kPa pressure [21]. Among the protein purifications, membranes prepared from PES have gained special importance as it provides high rigidity, a high degree of molecular immovability, and superior strength.

Conversely, membrane fouling is the major drawback faced by PES-based ultrafiltration membranes due to their hydrophobicity and surface roughness [31,32]. The adsorption and deposition of protein molecules on the membrane surface lead to the formation of a foulant layer. It is widely acknowledged that increasing hydrophilicity and decreasing surface roughness improve the membrane's antifouling characteristic properties [33]. Several roots have been adopted to enhance the separation characteristic properties of the PES membranes, which include surface coating, sulfonation, and blending with hydrophilic additives as (polyvinyl pyrrolidone (PVP), polyethylene glycols (PEG), polyethylene oxide (PEO)) [31,34,35].

On the other hand, the separation properties of a membrane are significantly influenced by surface pore size and cross-sectional morphology. The wet phase inversion process is the most extensively used technique for fabricating asymmetric membranes. The kinetic parameters such as solvent/non-solvent demixing rates and thermodynamic parameters, including polymer/additive-solvent interactions, were well controlled to obtain the desired membrane morphology and separation selectivity. Additionally, the polymer dope solution composition, coagulation bath temperature, and additive size alter the membrane morphology [36]. PEG has been used widely as a pore former due to its dispersion with membrane materials and is quite well miscible with solvents as well as non-solvents. Mohammad et al. investigated the effects of PEG concentrations, molecular weight, and coagulation bath temperature on the morphology of the PES membranes [37]. They found that the increasing PEG concentration, and PEG molecular weight (MW), increased the demixing rate of solvent/non-solvent and enabled the formation of macrovoids in the membrane structure. Lin et al. have studied the effect of different PEG molecular weights on ultrafiltration membrane properties and performance and found that the morphology of surface pore size increased with increasing PEG MW [38]. From the literature, the role of PEG as a pore former and the demixing rate has well understood in controlling the membrane morphology. However, limited articles have been reported on the rationalization of membrane morphology in the selective separation of CEW proteins.

The present study aims to develop hydrophilized and enhanced antifouling membranes to isolate Lysozyme from CEW. PES/sPES membranes with different porosities were fabricated using PEG (400 and 6000 kDa) additive and varying the coagulation bath temperature. The morphological changes of the prepared membranes were investigated using scanning electron microscopy (SEM), Atomic force microscopy (AFM), whereas the hydrophilicity of the membranes was evaluated using contact angle measurements. Subsequently, the performance of these membranes was investigated in obtaining pure Lysozyme under the optimized condition and antifouling properties.

2. Materials and methods

2.1. Materials

Polyethersulfone (PES) (35 kDa) and Polyethylene glycol (PEG) with MWCO 400 and 6000 Da polymers were procured from Solvay Specialties India Private Limited, Mumbai, India, for membrane synthesis and as pore-forming agents, respectively. Sulfuric acid, Triethyl phosphate ($C_6H_{15}O_4P$) (TEP), 1,1,2,2-tetrachloroethane ($C_2H_2Cl_4$), Methanol, N-Methyl-2-pyrrolidinone (NMP) chemicals were purchased from SD fine chemicals, Hyderabad, India. Dipotassium hydrogen phosphate (K_2HPO_4), Potassium dihydrogen orthophosphate (KH_2PO_4), Bradford reagent, Tris, Glycine, TEMED, Ammonium persulfate, Acrylamide, and Bis-acryl amide obtained from Sigma Aldrich, USA. The sodium hydroxide (NaOH), hydrochloric acid (HCl), and sodium chloride (NaCl) chemicals were procured from Avra Chemicals, Hyderabad, India. Coomassie blue staining solution was procured from Bio-Rad Laboratories (India) Private Limited, India, and used in Bradford protein assay to estimate protein concentration. The deionized water with TDS < 2 ppm was used for sample preparation and experimental studies in the laboratory using the RO membrane cascade system. The laboratory glassware, including burettes, conical flask, measuring jar, beakers, etc., for the preparation of solutions, was supplied by Borosil, Hyderabad, India.

2.2. Sulfonation of PES using Triethyl phosphate and Sulfuric acid

The sulfonated PES ultrafiltration (UF) membrane was prepared by phase inversion method using triethyl phosphate (TEP) and sulfuric acid, where TEP acts as a catalyst. The sulfonating agent was prepared using 5 ml triethyl phosphate in 10 ml sulfuric acid in a 1:2 ratio at 4°C and kept aside for 24 hours. On the other hand, 20 g of PES was dissolved in 100 ml of 1,1,2,2-tetrachloroethane at room temperature (27±2°C) [21] and continuously stirred at a rate of 450 RPM to get a homogenous solution. Then, 15 ml of the sulfonating agent was slowly added to the polymer solution at a 0.125 ml/min rate under continuous stirring at 75°C for 2 h (Scheme S1). The mixture was permitted to proceed for 120 minutes and terminated by precipitating the solution into an ice-cold bath. The precipitate was sieved and washed with methanol for 1 h, followed by drying at 65 °C under a hot air oven for 4 h. Further, to neutralize the SPES, the dried polymer was dissolved in 104 ml of 1-methyl-2-pyrrolidinone (NMP), as per the polymer weight. The dissolved polymer was precipitated into DI water followed by sieving and washing until reached neutral pH and dried at 70 °C for 20 h. This SPES polymer was used in the fabrication of ultra-porous cation exchange membranes.

2.3. Preparation of PES and SPES-UF membrane

PES and sPES membranes with different porosities were fabricated by the non-solvent-induced phase separation (NIPS) technique called the wet phase inversion process. NIPS technique is widely practiced to prepare various morphologies by controlling the thermodynamic characteristics of the demixing process. In the present study, the key preparation parameters are the type of additives and the temperatures of the coagulation bath. The additives such as PEG_400 and PEG_6000 Da were used as pore-forming agents, and a combination of varying coagulation bath temperatures was employed to enhance the pore density and control the pore size of the resulting membranes. Initially, 25 wt% of PES and SPES polymer solution were prepared by dissolving 25 g of polymer in 75 g of NMP and stirring for 4 h at room temperature (28±2°C). The obtained polymer solution was cast on a polyester (PE) non-woven fabric support using a doctor's blade with an air gap of 120 µm to achieve the desired membrane thickness. After that, the coated film was immediately immersed in DI water bath at a specified coagulation bath temperature. The same procedure was followed by adding 6% of PEG_400 or PEG_6000 additives to the polymeric solution and varying the non-solvent (DI water) bath temperature from 10 to 45°C to obtain various configurations. The combination of membrane denotations is provided in Table 1. The procedure for preparing PES and SPES membranes using the NIPS method is schematically represented in Fig. 1(a). The prepared membranes were washed thoroughly with DI water to remove the trace of solvent on the membrane surface and then dried at ambient conditions.

Table 1
Combinations of membrane fabrication

Membrane	ID	Polymer (g)	Additive, weight (g)	Solvent, weight (g)	Coagulation bath temperature (°C)
PES_25	M1	PES, 25	-	NMP, 75	25
sPES_25	M2	sPES, 25	-	NMP, 75	25
PES_PEG400_25	M3	PES, 25	PEG400, 1.5	NMP, 79.5	25
sPES_PEG400_25	M4	sPES, 25	PEG400, 1.5	NMP, 79.5	25
PES_PEG6000_25	M5	PES, 25	PEG6000, 1.5	NMP, 79.5	25
sPES_PEG6000_25	M6	sPES, 25	PEG6000, 1.5	NMP, 79.5	25
sPES_PEG400_10	M7	sPES, 25	PEG400, 1.5	NMP, 79.5	10
sPES_PEG400_45	M8	sPES, 25	PEG400, 1.5	NMP, 79.5	45
sPES_PEG6000_10	M9	sPES, 25	PEG6000, 1.5	NMP, 79.5	10
sPES_PEG6000_45	M10	sPES, 25	PEG6000, 1.5	NMP, 79.5	45

2.4. Phosphate Buffer preparation

In the present study, the phosphate buffer solution was prepared by mixing the dipotassium phosphate (A) and potassium dihydrogen phosphate solutions (B). Individual solutions of A and B are prepared by dissolving 87.09 g and 68.045 g in 500 ml DI water to obtain 0.5 L of 1M dipotassium phosphate and potassium dihydrogen phosphate, respectively. Further, to achieve a 7.4 pH of the buffer, 19.8 ml of solution A was added to 80.2 ml of solution B, followed by diluting 10 times to obtain 0.1 M phosphate buffer.

2.5. Egg white solution preparation

The supernatant egg white solution was prepared for the ultrafiltration process, where a 100 ml homogenized egg white was diluted with 900 ml of 0.1M phosphate buffer solution, filtered, and centrifuged at 12000 rpm for 15 min. The collected supernatant contains a lipid-free protein solution, a source for Lysozyme in the present study.

2.6. Experimental studies

2.6.1. Batch studies

Lysozyme extraction experiments were conducted to separate Lysozyme from egg white solution using PES and SPES-UF in dead-end and cross-flow filtration under batch mode operation. The supernatant solution of egg white was used as feed. The schematic representation of the batch mode experimental setup was shown in Fig. 1(b), where the feed tank of 5 L capacity was connected to the membrane module with a membrane-active surface area of 95 cm^2, through a peristaltic pump. The jacketed glass vessel was used as a feed tank to maintain the feed temperature. The permeate was collected at one end of the module and the reject was recycled back to the feed tank. The pressure gauge was fixed at the reject streamline to measure the applied pressure across the membrane. The pressure on the membrane surface was built by restricting the reject stream flow rate using a needle valve.

Before starting each experiment, the experimental setup was circulated with phosphate buffer to remove the previous experimental traces from the system. The jacketed feed tank was filled with the prepared egg white solution as feed, which was maintained at 10 ± 2 °C temperature with the help of coolant circulation. The feed was fed to the membrane module in two different configurations of dead-end and cross-flow manner at 120 rpm with 15 psi pressure. In dead-end filtration, the feed flow is perpendicular to the membrane surface, whereas, in cross-flow filtration, the feed flows parallel to the membrane surface. The permeation flux was estimated by measuring the volumetric flow rate of permeate and samples were analyzed qualitatively and quantitatively. The initial screening of the synthesized membrane was done in batch mode experiments, where the separation characteristics such as permeation flux, hydraulic resistance, and protein concentration in permeate were estimated. Further, experiments were carried out to test the robustness of membrane performance in the continuous extraction of Lysozyme in semi-batch mode.
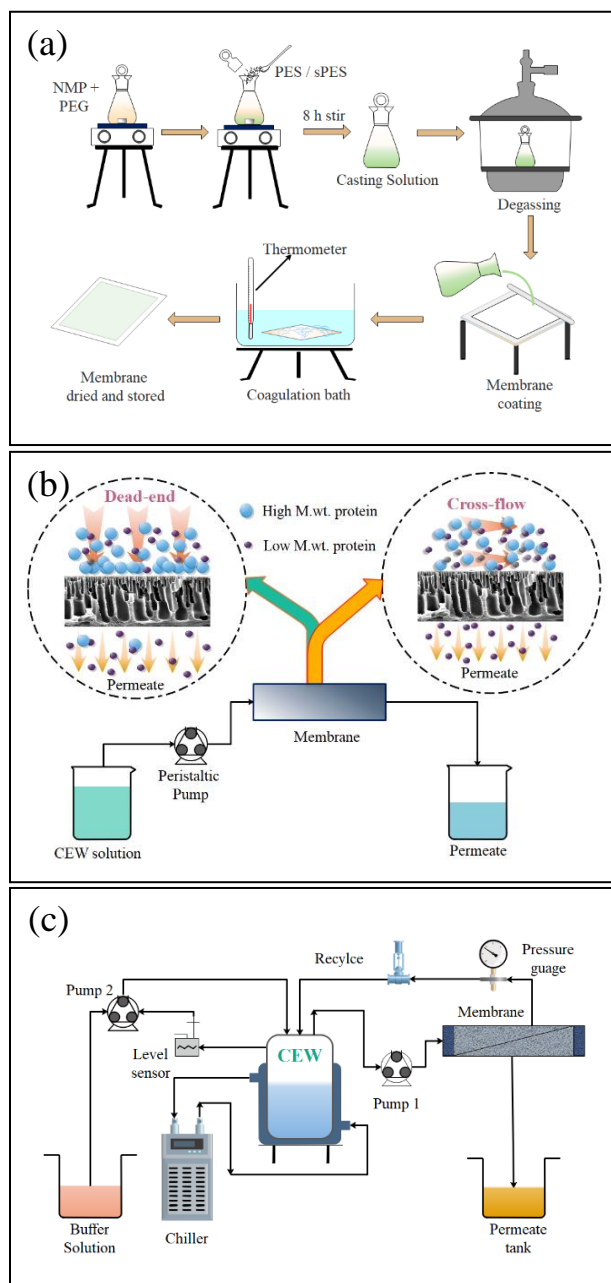
Fig. 1. Schematic representation of **(a)** fabrication of PES/sPES membranes, **(b)** dead-end and cross-flow mode of ultrafiltration, **(c)** semi-batch operation for continuous extraction of Lysozyme from CEW.

2.6.2. Semi-batch studies

The semi-batch experiments were conducted to continuously extract Lysozyme from the feed egg white solution. The semi-batch studies were performed with the selected membrane from the preliminary screening based on selective separation of Lysozyme under bench-scale. The schematic of the semi-batch mode ultrafiltration system was provided in Fig. 1(c), where an additional buffer solution tank was introduced to the feed tank of the batch mode experimental setup. The buffer solution was continuously added to the feed tank in order to maintain the constant feed volume. The feed tank level was continuously monitored using a level sensor, which activates the buffer feeding pump (pump 2).

2.6.3. Protein Adsorption studies

The protein adsorption experiments were performed to ascertain the adsorbed amount of protein on the membranes. These experiments were conducted by submerging the membranes in a supernatant solution. Rectangular pieces of membranes ($24cm^2$ area) were engulfed in vials containing 40g of egg white supernatant solution (10-fold) in 0.1M phosphate buffer of pH = 7.4. The vials were then kept on the shaker at 120 RPM at room temperature (RT) with constant stirring. Then for every 24 h, the supernatant solution was collected until the membranes got saturated and the concentration of protein in the supernatant solutions was determined using a UV-Vis spectrophotometer at 280 nm. The amounts of protein adsorbed on the membranes were estimated from the change in UV absorption of protein in the supernatant solution before and after the adsorption. The final results are the average of three measurements for each membrane [39].

2.7. Membrane characterization

2.7.1. FTIR

The surface chemistry of chemical bonds and functional groups of the PES/sPES membrane before and after protein adsorption were examined by Fourier transform infrared spectroscopy (FT-IR) using a PerkinElmer spectrum 100 FTIR spectrophotometer, Boston, MA, USA. The spectrum was measured in the wavelength region of 650 – 4000 cm^{-1} at ambient temperature.

2.7.2. SEM

The cross-sectional morphology of neat PES/sPES and PEG-loaded membranes were analyzed by scanning electron microscopy (SEM) with Quanta 200 model SEM instrument. Before the SEM analysis, the membranes were freeze fractured in liquid nitrogen to shield the cross-sectional morphologies and then coated with iridium of 5 nm thickness to minimize surface charging.

2.7.3. AFM topography

The three-dimensional surface topographical changes of prepared membranes were analyzed using atomic force microscopy (AFM, Asylum Research MFP-3D Infinity). The relative surface roughness of the membranes was collected by examining the membrane with a resolution of 256 x 256 and a scanning area of 5 X 5 µm under tapping mode.

2.7.4. Contact angle (CA) measurement

The wetting ability of the PES/sPES membranes' surface was characterized using Dino-Lite Basic AM211 digital microscope model CA analyzer, Taiwan. The CA measurements were performed at 25 °C using the sessile drop method by placing a 3-µL droplet of water on the dry membrane sample; noted within 5 s after dropping to achieve accurate values.

2.7.5. Porosity

To estimate the bulk porosity of the membranes, firstly, the sample membranes (10 x 10 mm) were soaked in deionized water for about 24 h. Later, the leftover water droplets on the surface were wiped off with soft tissue and measured using a balance. Successively, the samples were dried in a hot air oven maintained at 60 °C for 8 h to diminish the upshot of lasting additives and solvents on porosity measurement. The corresponding weights of dry membranes were recorded. The bulk porosity (ε) of the primed membranes was estimated by a most regularly used gravimetric method (Equation 1) [40].

$$\varepsilon = \frac{W_w - W_d}{\rho_w \times A \times \delta} \times 100 \tag{1}$$

where, W_w and W_d are weights of wet and dry membranes in g, ρ_w is the density of water in g/cm^3, A is the membrane-active surface area in cm^2, and δ is the membrane thickness in cm.

2.7.6. Pure water flux (PWF) and fouling studies

All the membranes synthesized were analyzed for their performance and fouling characteristics based on the pure water flux. At first, the permeation test was performed by passing DI water through the membrane sample at 20 psi, and the time taken for collecting every 10 mL of permeate was recorded. In general, fouling studies are carried out to govern the life period of the membranes. The sample membranes were primarily immersed in egg white supernatant for 7 days to investigate the antifouling behavior. After that, the membranes were cleaned with DI water, and the pure water permeation test was carried out similarly. The pure water flux through the membranes is calculated using Equation 2.

$$J_w = \frac{Q}{A} \tag{2}$$

where, J_w is the pure water flux (L/m^2.h), Q is the permeate volumetric flow rate (L/h) and A is the effective area of the membrane (m^2).

2.7.7. Hydraulic resistance

Hydraulic resistance is a key element that defines the productivity of any pressure-driven membrane process. The membrane performance at different operating pressures and its optimization are important factors for ultrafiltration operations. The hydraulic resistance exerted by the membrane (Rm) is an intrinsic property determined by pure water flux. Hydraulic resistance is assessed by first plotting the pure water flux as a function of transmembrane pressure. The slope of this curve gives the ratio of water flux to the transmembrane pressure that states the hydraulic permeability, and the inverse of it describes the hydraulic resistance of the membrane. The relation of hydraulic resistance in terms of flux and pressure is shown in Equation 3.

$$R_m = \frac{P_T}{J_w \mu} \tag{3}$$

where R_m is membrane hydraulic resistance (m^{-1}), P_T is the transmembrane pressure (N/m^2), and μ is the DI water viscosity (N.s/m^2).

2.7.8. Ion Exchange Capacity (IEC)

To evaluate the ion exchange capacity (IEC), the sample membrane of 10 x 10 cm^2 was immersed in 1 mol/dm^3 HCl solution. Then, the excess HCl was thoroughly removed by washing the membrane with DI water. Subsequently, the sample was dipped in 1 mol/dm^3 NaCl solution, where the protons were replaced with the Na$^+$ ion on the membrane surface. The released protons from the membrane were estimated by titrating with NaOH solution (0.01 mol/dm^3), where phenolphthalein was used as an indicator. Afterward, the membrane was washed with DI water and dried by placing it in the oven maintained at 50 °C for about 10 h. The weight of the dry membrane was measured, and then the IEC was estimated using Equation 4.

$$IEC = \frac{C_{NaOH} \times V_{NaOH}}{W_{dry}} \tag{4}$$

where C and V are the concentration (mol/dm^3) and volume consumed (dm^3) of NaOH, respectively, and W_{dry} is the membrane dry weight (g).

2.8. Analytical Studies

2.8.1. SDS-PAGE for characterization

The SDS–PAGE was performed using 12% polyacrylamide gel. The polyacrylamide gel was made by adding resolving gel (pH–8.8; 5ml) and stacking gels (pH -6.8; 2ml). First, the resolving gel (pH–8.8) was prepared by adding 1575µl water, 2000µl ABA(Acrylamide/Bis-acrylamide) (30% acrylamide), 1300µl Tris buffer (pH–8.8), 50µl Sodium Dodecyl Sulphate (SDS; 10%), 50µl Ammonium Persulfate (10%), 25µl stain free and 2µl TEMED (N, N,N′,N′-Tetramethyl ethylenediamine) and it was poured in between plates. Afterward, 2ml stacking gel was prepared by adding 1400µl water, 330µl ABA (30% acrylamide), 250µl Tris buffer (pH – 6.8), 20µl SDS (10%), 20 µl APS (10%) and 2µl TEMED and it was also poured above the resolving gel. Then 30µl sample was added to the 10µl loading dye and heated at 100°C for 10 min for protein denaturation. Afterward, the samples were loaded on a prepared polyacrylamide gel and an experiment was

performed. After that, the gel was kept on UV light to detect protein. Then the gel was stained, and after some time, it was de-stained to identify the protein.

2.8.2. Bradford protein assay

In the Bradford protein assay *[41]*, the protein concentrations in each sample were prepared by adding 1µl of each protein sample in 99µl water. After that, 100µl Bradford reagent was added to each sample. A blank was prepared by adding 100µl water and 100µl Bradford reagent as reference. After 2 minutes, the absorbance of each sample was recorded using spectrophotometrically at 562 nm. The protein concentration was calculated from the standard curve prepared using bovine serum albumin as standard.

3. Results and discussion

3.1. FT-IR characterization

Fig. S1 Shows the FTIR spectra of PES and sPES. From the FT-IR spectra, the signals at 1,072, 1578, and 2923 cm^{-1} were attributed to aromatic C-C stretching and bending along with C-H stretching vibrations, respectively, commonly found in polyethersulfone [42,43]. The asymmetric and symmetric stretching vibrations of sulfone (O=S=O) group signals were observed at 1,298 and 1148, whereas the asymmetric aryl ether (C–O–C) was identified at 1,237, respectively. Additional shoulder appeared at 1,027 cm^{-1}, representing the characteristic peak of the symmetric aromatic -SO$_3$H stretching vibrations, consistent with the results reported by Noel Jacob et al. [42]. With the introduction of the -SO$_3$H group on the aromatic ring during the sulfonation, a change in C=C stretching vibration appeared at 1,662, which confirms the substitution of the sulfone group on the benzene ring.

3.2. Preparation conditions and membrane structures

In the present work, various porosity membranes were fabricated using the non-solvent-induced phase separation (NIPS) method for the selective separation of Lysozyme from CEW. Generally, the membrane's physical morphology and porosity strongly depend on the cast conditions, including solvent/non-solvent demixing rate, additives, cast film thickness, and viscosity of the cast solution. Several studies have been reported to prepare different morphologies of the membrane by controlling the thermodynamics of the demixing rate [44,45]. The coagulation bath temperature gives excellent flexibility in altering the demixing rates; the higher the temperature, the higher the demixing rate, which leads to wide pore diameters and vice-versa. On the other hand, the size of the additive also influences the morphology of the resulting membrane. To understand the influence of the additive size, two different molecular weight PEG (400, 6000) solutions were employed as a pore-forming agent during the membrane preparation. To control the demixing rate, the non-solvent coagulation bath temperature was varied from 10 - 45 °C.

3.2.1. Effect of pore-former on PES and sPES membranes

The microscopic and topographic morphologies were obtained using SEM and AFM to investigate morphological changes of PES and sPES membranes in the presence and absence of PEG additives, which were cast at ambient temperature. The cross-sectional morphology and corresponding surface topographic images of the prepared membranes are presented in Fig. 2(a-f). Fig. 2(a),(b) represents the morphology of neat PES followed by sPES membranes, whereas Fig. 2(c),(d), and (e),(f) show the morphological changes between PES and sPES membranes in the presence of PEG400 and PEG6000 additive, respectively.

The cross-sectional morphology of the PES and sPES membranes cast in ambient conditions resulted in a similar asymmetric structure comprising two distinguished micro and macro void layers. The asymmetric structure of the neat PES and sPES membrane exhibited a typical length of microvoids ranging from 10 – 12 µm above the finger-like macro void layer. Apart from similar morphological features of the membranes, the top microporous layer displayed variation in the average pore diameter, which is summarized in Table 2. On the other hand, the porosity of the membranes was estimated using both gravimetric and cross-sectional SEM image analysis. The detailed procedure for the porosity measurements was done by image processing using ImageJ software as reported by Sun et al. [46]. The estimated % porosity of the membranes is summarized in Table 2. It can be observed that there is a noticeable difference in the percentage porosities assessed by the gravimetric method and ImageJ tool, besides heeding commensurate trends of divergence. Conventionally, in gravimetric analysis, the total void volume of a membrane is indirectly measured with the occupied volume of the pore-wetting agent

(water) and it was assumed that the entire void volume is filled with a wetting agent. However, the estimated void volume using this technique deviates from the true void volumes. This analysis at times provides porosity estimates to large magnitude for membranes showing ample hydrophilic nature, while it underestimates for the partial hydrophobic membranes. On the other hand, the digital image processing tool gives realistic porosity values by skimming the high-resolution SEM images. As such it considers the actual geometry of the pores irrespective of the membrane characteristics such as hydrophilicity, hydrophobicity, and membrane swelling. Overall, the ImageJ tool is a relatively accurate model for estimating porosity. From overall observations of cross-sectional morphology and porosity of neat membranes, the sPES displays approximately identical features to that of PES.

The morphologies of the additive doped membranes prepared from 6 wt% of PEG400 (Fig. 2(c) and (d)) and PEG6000 (Fig. 2(e) and (f)) revealed significant development in the pore structure. In the presence of PEG pore former, the asymmetric morphology of PES and sPES membranes led to a symmetric structure. In general, the addition of various types of pore-forming agents results in considerable changes in bulk morphology and porosity compared to neat polymeric membranes [47]. The hydrophilic PEG additive plays an important role in enhancing porosity, where increased pore diameters and reduced length of the microporous layer have been observed. Especially in the case of PEG6000 microporous layer almost disappeared, which led to symmetric pore stretching throughout the cross-section. The maximum % porosity was achieved for PES and sPES membranes prepared in the presence of PEG400 and found to be 70.10 and 72.11, respectively. Additionally, increased cross-sectional pore diameters were observed due to the high demixing rate of PEG with water.

Contact angles of PES and sPES membrane were measured to evaluate the surface wettability and hydrophilic interactions, which directly correlated to the effect on the pure water flux (PWF) and antifouling tendency [48]. A reduction in the contact angle indicates an increase in the hydrophilicity of the membrane surface. Certainly, neat PES is known to be a hydrophobic polymer and tends to foul quickly. The measured contact angles are illustrated in Fig. 2(g). The contact angles of neat PES (M1) and sPES (M2) were found to be 81.2º and 71.7º, respectively. The reduction in the contact angle of sPES compared to the PES can be attributed to the presence of sulfone functional (-SO$_3$H) groups on the membrane surface. The sulfone group exhibits strong hydrogen bonding and Van der Waals interactions with polar groups [42,49]. From Fig. 2(g), it is clearly evident that there is a significant decrease in the contact angle of PES and sPES membranes in the presence of a PEG additive. The surface porosity ascribes to the increase in the hydrophilicity of PEG-doped membranes. Noel Jacob et al., studied the effect of PEG200 additive on the PSf/SPES blend membranes. Their study revealed that the surface porosity of the membranes has a strong effect on the contact angle due to capillary force acting underneath the water drop, which leads to penetration [42]. Furthermore, the lowest contact angle of 65.8º was observed for the sPES membrane cast in the presence of PEG400. Therefore, sPES membranes demonstrate increased hydrophilicity compared to the PES membranes, and low fouling tendency [42,48].

The three-dimensional surface topographic analysis and roughness parameters of the PES and sPES membranes were characterized using AFM mapping. The surface roughness parameters such as mean roughness (S_a), RMS roughness (S_q), and Maximum grain size height (S_z) are essential to assess the fouling tendency of the prepared membranes for protein purification [48]. The roughness factors of the AFM images were analyzed using Gwyddion (version 2.60), a modular program used for data visualization and analysis of SPM (scanning probe microscopy) images. The relative surface parameters of the membranes were investigated in a 5 x 5 µm^2 area of membranes and are summarized in Table 2. From Fig. 2(a) and (b) and Table 2, it can be observed that the relative roughness of the sPES has decreased when compared to the neat PES membrane. This may be because the sulfonic acid groups present on the sPES exhibited strong hydrophilic interaction during the phase inversion [50]. Wen et al. fabricated antifouling PES ultrafiltration membranes by blending sulfonated polysulfone (sPSf) as a copolymer. Their study found that the roughness of the blend membranes exhibited a decreased trend as the degree of sulfonation increased. On the other hand, it also recognized that incorporating additives in the dope solutions would increase the surface roughness of the prepared membranes compared to the neat polymer [33,36,47,48]. However, the sPES_PEG400_25 membrane exhibited much lower surface roughness than that of other PEG-doped membranes. Whereas the PEG6000 loaded PES and sPES membranes demonstrated higher surface roughness, which would have high tendency of surface fouling.
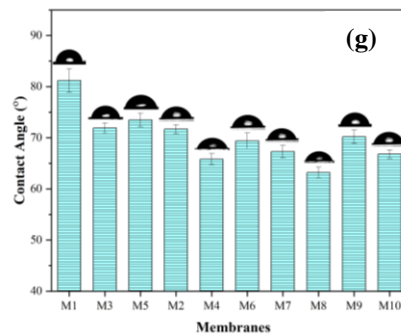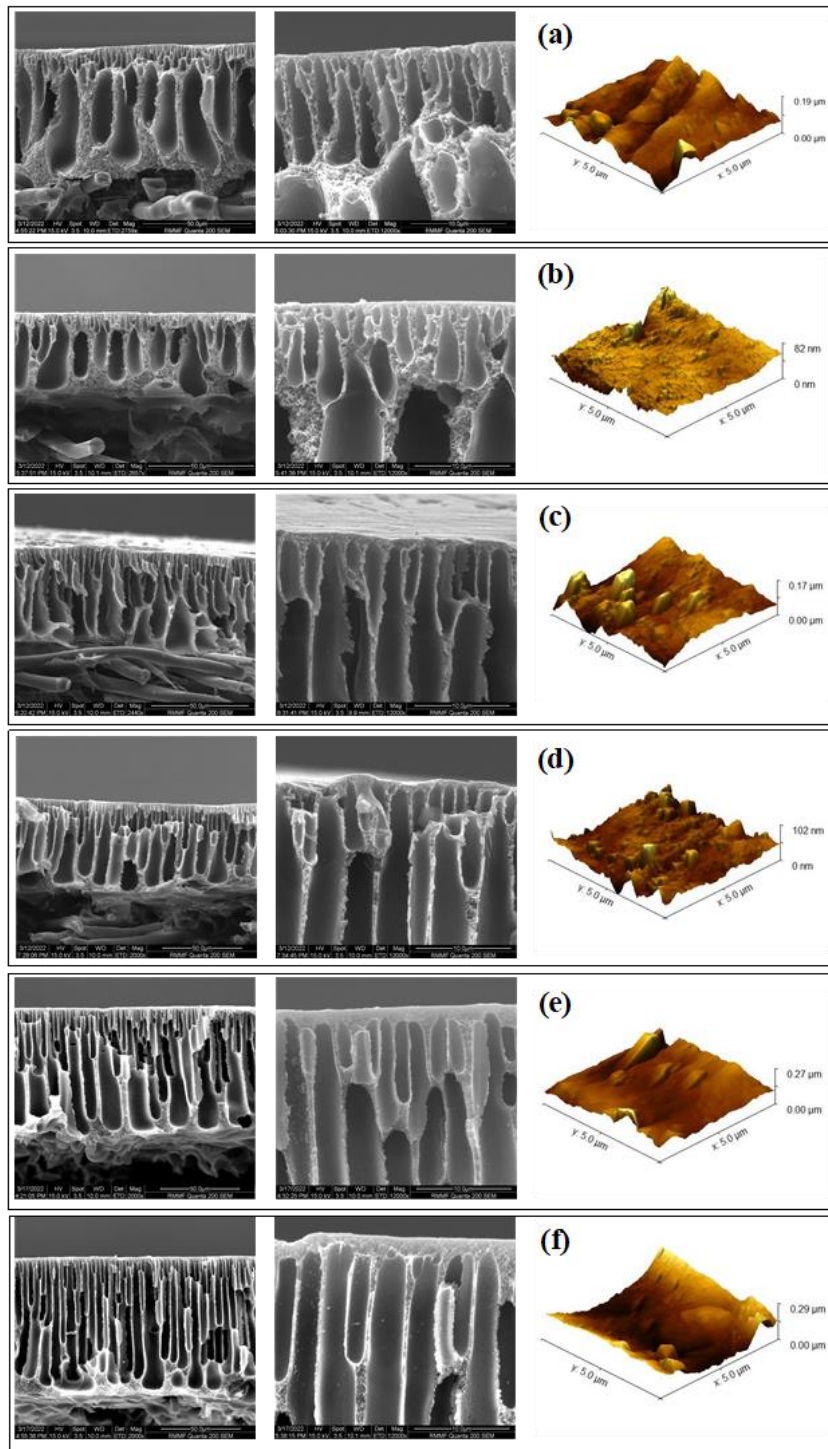
Fig. 2. The cross-sectional morphology and corresponding surface topographic images of PES/sPES membranes **(a)** M1, **(b)** M2, **(c)** M3, **(d)** M4, **(e)** M5, and **(f)** M6, **(g)** Static water contact angles of the PES and sPES membranes.

Table 2
Porosity and roughness parameters of the PES and sPES membranes

Membrane	Avg top layer micro void diameter (μm)	Porosity (ε, %)		Roughness (nm)		
		Gravimetric	Image analysis	S_a	S_q	S_z
PES (M1)	1.44 ± 0.41	43.56	63.91	14.99	21.14	193.0
PES_PEG400_25 (M3)	2.61 ± 0.80	63.32	70.10	16.27	22.10	171.3
PES_PEG6000_25 (M5)	2.73 ± 0.99	58.56	68.22	21.54	29.73	266.9
sPES (M2)	1.75 ± 0.66	45.23	66.82	5.76	7.93	81.7
sPES_PEG400_25 (M4)	3.01 ± 0.74	68.23	72.11	8.27	11.05	102.0
sPES_PEG6000_25 (M6)	2.76 ± 0.73	58.33	69.42	50.74	59.81	442.5

3.2.2. Effect of coagulation bath temperature

Another influencing parameter on the membrane morphology is the coagulation bath conditions. The demixing rate of solvent and non-solvent rates could be precisely controlled by changing the temperature condition of the non-solvent bath. Cross-sectional SEM images of sPES membranes cast in the presence of PEG additives and coagulation bath temperatures of 10 and 45 °C are presented in Fig. 3. As per Fig. 3(a)-(d), the rise in coagulation bath temperature from 10 °C to 45 °C ensued in giant macro voids formation. Furthermore, it was noticed that the membrane cast in the coagulation bath temperature of 10 °C resulted in an asymmetric structure with micro and macro void layers due to the slow demixing rates. On the other hand, the membranes fabricated at 45 °C created larger macro void volumes within the bulk matrix of the membranes under the influence of rapid demixing phenomena [45]. In contrast, at lower temperatures, due to the slow demixing rates initially leading to a formation of a tighter microporous layer afterward, the nucleation occurs slowly in the bulk matrix. Consequently, the membranes cast at lower temperatures despite the presence of PEG additives tend to form an asymmetric layer throughout the cross-section. These results are in good agreement with the previous reports [36,44,45,51].

3.3. Performance evaluation using PWF and hydraulic resistance

The PWF is one of the vital characterizations to demonstrate the morphological changes in the performance of prepared membranes. The calculated PWF and corresponding hydraulic resistance of the M1-M10 membranes are summarized in Table 3. PWF of the neat PES membrane exhibits a very low value of 5.67 Lm^{-2}h^{-1}bar^{-1}, whereas the neat sPES demonstrated 20.50 Lm^{-2}h^{-1}bar^{-1}. Although both neat membranes have similar asymmetric morphology, sPES showed higher PWF than the PES membrane. The increase in the PWF was attributed to the higher hydrophilic character of the sulfone groups of sPES, confirmed by the contact angle analysis. Table 3 shows significant enhancement in the PWF of PES and sPES membranes when cast in the presence of a PEG additive at ambient conditions (i.e., M3-M6). Furthermore, the membranes fabricated in the presence of PEG400 showed higher PWF compared to the PEG6000 due to the higher porosity and hydrophilic characteristic property.

On the other hand, the sPES membrane, when cast at temperatures of 10 to 45°C in the presence of PEG400 and PEG6000, shows PWF values of 73.57, 107.46, 167.98 L m^{-2}h^{-1}bar^{-1} and 57.23, 63.10, 153.81 L m^{-2}h^{-1}bar^{-1}, respectively, indicating a rise in PWF values with increase in coagulation bath temperature. The observed trend in PWF values is consistent with the morphological analysis of SEM images presented in section 3.2. As the temperature of the coagulation bath increases, the formation of macro voids increases due to high demixing rates [44]. Consequently, the hydraulic resistance of pure water permeation decreases with the increase in the porosity of the membranes (Table 1).

3.4. Ion exchange capacity (IEC) of PES and sPES membranes

IEC is an essential factor for analyzing the charge density of a membrane. In the present study, the IEC values of the prepared membranes were estimated using the titration method described elsewhere [52]. The calculated IEC values are presented in Table 3. IEC of the membrane cast from neat PES and PES/PEG blend membranes were considerably constant and exhibited a value of 0.04 ± 0.01, consistent with the value presented by Klaysom et al. [52]. In contrast, the IEC values of the sPES and sPES/PEG blend membranes showed a significant difference and increased with the increase in the porosity of the membrane. The enhanced IEC of the sPES membranes might be attributed to the exposure of an expanded number of sulfonated groups when the porosity of the membrane increases. The maximum IEC was found to be 1.137 mmol eq/g for the membrane cast from sPES with PEG400 at a coagulation bath temperature of 45 °C (M8). Due to -SO$_3$- groups of the

sulfonated PES possessing a negative charge, IEC values of the sPES membrane indicate surface charge negativity. Subsequently, the negatively charged surface membranes show affinity towards the positively charged protein during the separation. In addition, the high molecular weight proteins with a negative charge will show a low tendency of fouling on the negatively charged membranes [50].
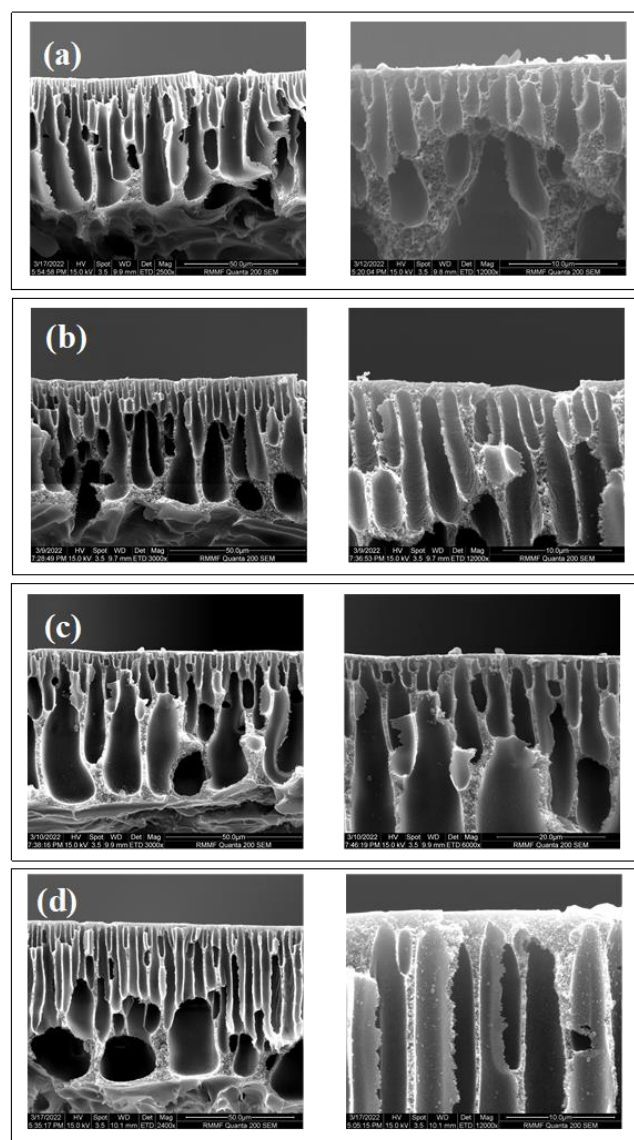

Fig. 3. Cross-sectional SEM images of sPES membranes cast in the presence of PEG additives and coagulation bath temperatures of 10 and 45 °C (a) M7, (b) M8, (c) M9, and (d) M10

Table 3
PWF, Hydraulic resistance, and IEC values of PES and sPES membranes

Membrane	PWF (L m^{-2}h^{-1}bar^{-1})	Hydraulic resistance R$_m$ (x 10^{12} m^{-1})	IEC (mmol eq/g)
PES_25 (M1)	5.67	98.37	0.030
sPES_25 (M2)	20.50	27.20	0.625
PES_PEG400_25 (M3)	10.93	51.00	0.040
sPES_PEG400_25 (M4)	107.46	5.19	0.854
PES_PEG6000_25 (M5)	9.46	58.96	0.045
sPES_PEG6000_25 (M6)	63.10	8.83	0.656
sPES_PEG400_10 (M7)	73.57	7.58	0.540
sPES_PEG400_45 (M8)	167.98	3.32	1.137
sPES_PEG6000_10 (M9)	57.23	9.74	0.477
sPES_PEG6000_45 (M10)	153.81	3.62	0.757

3.5. Lysozyme separation from CEW

CEW solution was chosen as a source for the isolation of Lysozyme, which is the most acceptable and naturally available. However, the isolation of Lysozyme from CEW is challenging as the concentration of Lysozyme is minimal among the CEW proteins. The major protein components of CEW and properties such as molecular weight and iso-electric points are presented in Table S1. Ovalbumin, Ovotransferrin, and Ovomucoid are high molecular weight proteins compared to Lysozyme and are the major contributors of CEW proteins, comprising about 54%, 12%, and 11% of the total proteins, respectively [5]. Lysozyme and Ovomucoin are present at approximately 3.5 % of each in the total protein [23].

In ion-exchange column chromatography and pH-graded gel, a protein can be separated from a crude mixture based on the difference in the iso-electric points. The iso-electric point of a protein indicates the pH value where the protein has a neutral net charge (zero). At the same time, protein carries a net negative charge above the iso-electric point and vice-versa [5]. Moreover, it is also reported that the iso-electric points play an essential role in the adsorption process where the pH conditions strongly influence the adsorption capacity of the substrate [5,39]. From Table S1, the iso-electric points of higher molecular weight proteins in the CEW are less than 6.1, besides Lysozyme being 10.7 [53]. Chang et al. studied the effect of pH on the batch adsorption of Lysozyme from CEW at pH ranging from 4 to 12. The results revealed that the adsorption selectivities of hydrolyzed polyacrylonitrile (PAN-COOH) and bromoacetic acid functionalized polyacrylonitrile (PAN-BrA) electrospun fibers at pH 9 presented 2.37 and 2.43 folds, relatively higher than at pH 5, respectively. Similarly, Fang et al. studied the batch adsorption capacity of sulfonated polysulfone membranes at pH 7.4 for selective adsorption of synthetic Lysozyme solutions [39]. Table S1 shows that Lysozyme possesses a net positive charge in phosphate buffer with a pH of 7.4, while higher molecular weight proteins (Ovalbumin, Ovotransferrin, and Ovomucoid) have a net negative charge. Thus, pH 7.4 was chosen as the buffer media for the CEW crude mixture during the isolation of Lysozyme through affinity base ultrafiltration. The strategic approach effectively separates and minimizes the protein accumulation on the membrane surface due to the electrostatic repulsion.

3.5.1. Effect of flow patterns on the Lysozyme extraction from CEW

The ultrafiltration experiments were carried out in the dead-end and cross-flow configurations to assess the membrane performance in the isolation of Lysozyme from CEW. Fig. 4(a) shows the flux values of M1-M10 membranes, and Fig. 4(b) represents the corresponding total protein concentration in the permeate. Additionally, sodium dodecyl sulfate-polyacrylamide gel electrophoresis (SDS-PAGE) analysis was performed to qualitatively analyze dead-end (Fig. 4(c)) and cross-flow (Fig. 4(d)) permeate samples. Fig. 4(a) shows that in membrane M1-M10, the permeation flux is enhanced when operated under a cross-flow configuration compared to the dead-end filtration. This is because the cross-flow pattern of feed significantly reduces the concentration polarization of high molecular weight protein on the surface of the membrane [54]. The flow direction in cross-flow filtration is parallel to the membrane surface, whereas it is perpendicular in dead-end filtration. The perpendicular flow of feed accumulates the retained proteins on the membrane surface, leading to a fall in the permeation flux. Furthermore, it is also recognized that dead-end flow filtration has a high fouling tendency compared to the cross-flow configuration [55]. Additionally, the flux of the

sPES membranes is significantly improved compared with PES membranes. As we discussed in section 3.2.1., the hydrophilicity and electrostatic interaction of proteins with the sulfonic functional groups of the sPES improved the permeation flux compared to the PES.

On the other hand, the total protein content in the permeate significantly varied from M1-M10 along with the difference in the feed flow patterns (Fig. 4(b)). From the visual observation of Fig. 4(b), the total protein content of permeate samples collected from M4, M6, M8, and M10 membranes is relatively high compared to the rest of the membranes. However, the protein concentration estimated from the Bradford assay does not reveal permeation quality. Thus, the samples were analyzed using the electrophoresis technique. The results in SDS-PAGE, which are presented in Fig. 4(c) and (d), reveal that the high total protein in the permeate sample of M6, M8, and M10 is due to the presence of Ovalbumin and Overtransferrin (clear broad bands has been observed). As discussed earlier, M8 and M10 were cast under 45 °C due to the high demixing rates of solvent/PEG additive with the non-solvent resulting in wider surface pores. Whereas the morphological changes of M4 (Fig. 2(d)) and M6 (Fig. 2(f)) significantly influence the size of the PEG additive. From the above CEW permeation flux and protein analysis, it can be concluded that the membrane cast in the presence of PEG6000 fails to retain higher molecular weight proteins. In contrast, the protein band of Ovalbumin and Overtransferrin in the permeate of the M4 membrane is found to be relatively small and almost disappeared when operated under cross-flow filtration. It is noteworthy that the permeate samples of the dead-end and cross-flow modes were collected after one hour after the start of the operation. During the course, feed volume is decreased as the permeate is collected, leading to an increase in the viscosity and concentration of total protein. To minimize the feed concentration fluctuation on the M4 membrane performance, a semi-batch model was configured where the feed volume is maintained constant.

3.5.2. Semi-batch mode isolation of Lysozyme

As described above, the ultrafiltration experiment of the M4 membrane was performed by maintaining the constant feed volume. The SDS-PAGE of permeate samples collected in the 30 min of time intervals are shown in Fig. 4 (e). Remarkably, at constant feed volume, the dynamic permeation of the M4 membrane demonstrated selective separation of Lysozyme from the complex CEW solution. Notably, the membrane morphology and electrostatic interaction between surface and protein are rationally correlated. At pH 7.4, the negatively charged high molecular weight proteins have weaker interaction with the negatively charged M4 surface and prevent permeation through the membrane. The clear and thick 14 kDa band of continuously extracted permeate sample indicates successful isolation of Lysozyme with the membrane fabricated using sPES/PEG400 under ambient coagulation conditions. Hence, the morphology of the membrane with the conjugated effect of electrostatic interactions and optimization of the extraction process led to the high purity of Lysozyme in the permeate.

3.6. Protein adsorption studies and membrane fouling evaluation

The antifouling performance of PES/sPES membranes was assessed using PWF analysis and protein adsorption. Fig. 5(a) shows that the PWF of M1-M10 membranes after soaking for 7 days in the supernatant CEW solution significantly decreased due to the deposition of proteins on the membrane surface. Furthermore, the relative change in protein concentration in the supernatant during the static adsorption of membranes is illustrated on the secondary axis of Fig. 5(a). The PES membranes adsorbed a considerable amount of protein on the membrane surface, clearly evident from the reduction in the supernatant protein concentration (Fig. 5(a)), whereas the protein uptake on the sPES membranes was minimal. Briefly, the fouling tendency of sPES is lower than that of PES membranes. It has to be noted that the surface roughness and hydrophilicity of membrane and electrostatic interactions with proteins are the primary factors responsible for the antifouling characteristics [36,43]. Topographic (Fig. 5(b) and (c)) and surface morphologies (Fig. 5(d) and (e)) of M1 and M4 membranes, revealed the formation of protein layer. The AFM topography showed that the neat PES heavily adsorbed protein, whereas the sPES (M4) exhibited a low adsorption tendency. As discussed earlier in section 3.2.1., the surface roughness of the sPES membranes is substantially lower than the PES. Additionally, electrostatic repulsion force is offered between the negative charge of sulfonic groups with the negatively charged proteins, which further reduces the fouling tendency of sPES membranes.
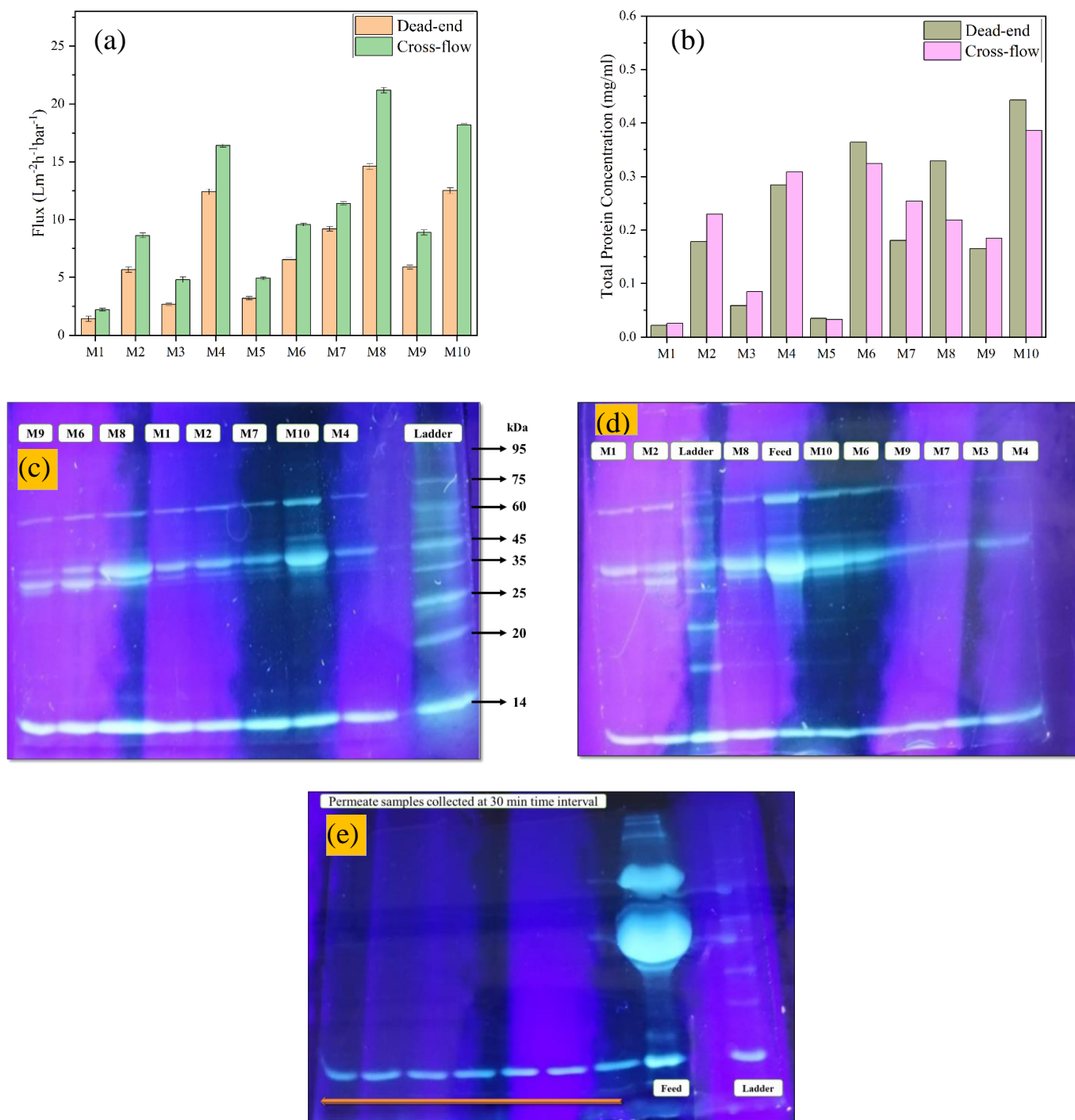
Fig. 4. Purification of Lysozyme from CEW crude solution using PES/sPES membranes **(a)** Permeation flux, **(b)** total protein, SDS-PAGE analysis of **(c)** dead-end, **(d)** cross-flow permeate, and **(e)** Evaluation of Lysozyme purity under semi-batch mode

A more comparative and deeper understanding of the foulant layer on the membranes were analyzed using EDS mapping (Fig. 5(f) and (g)) and ATR-FTIR analysis (Fig. 5(h)). Gorzalski et al. studied elemental analysis of the foulant layer using energy-dispersive X-ray spectroscopy (EDS), Rutherford's backscattering spectrometry (RBS), and X-ray photoelectron spectroscopy (XPS) evaluated whether the three techniques yielded consistent results for fouled membrane composition [56] and recommended that EDS as an appropriate method to evaluate the overall elemental composition of the foulant layer. The results obtained from EDS were consistent with the SEM and AFM analysis, where the protein adsorbed spots were enriched with calcium (Ca) and oxygen elements [56]. However, the elemental mapping of M4 showed a lower intensity of fouled layer. In order to understand the fouling tendency of sPES membranes, ATR-FTIR spectra were collected to identify the functional groups of the adsorbed protein [57]. Fig. 5(h) illustrated functional group stretching at 1660-1670 cm^{-1}, 1547 cm^{-1} of Amide I and Amide II of the adsorbed CEW proteins [58]. Furthermore, ATR-FTIR is a semi-quantitative technique that provides information on the amount of protein adsorbed on the membrane surface. It is evident that the M4 membrane indicates a low binding of protein compared to that of M2, M6, M8, and M10 membranes.
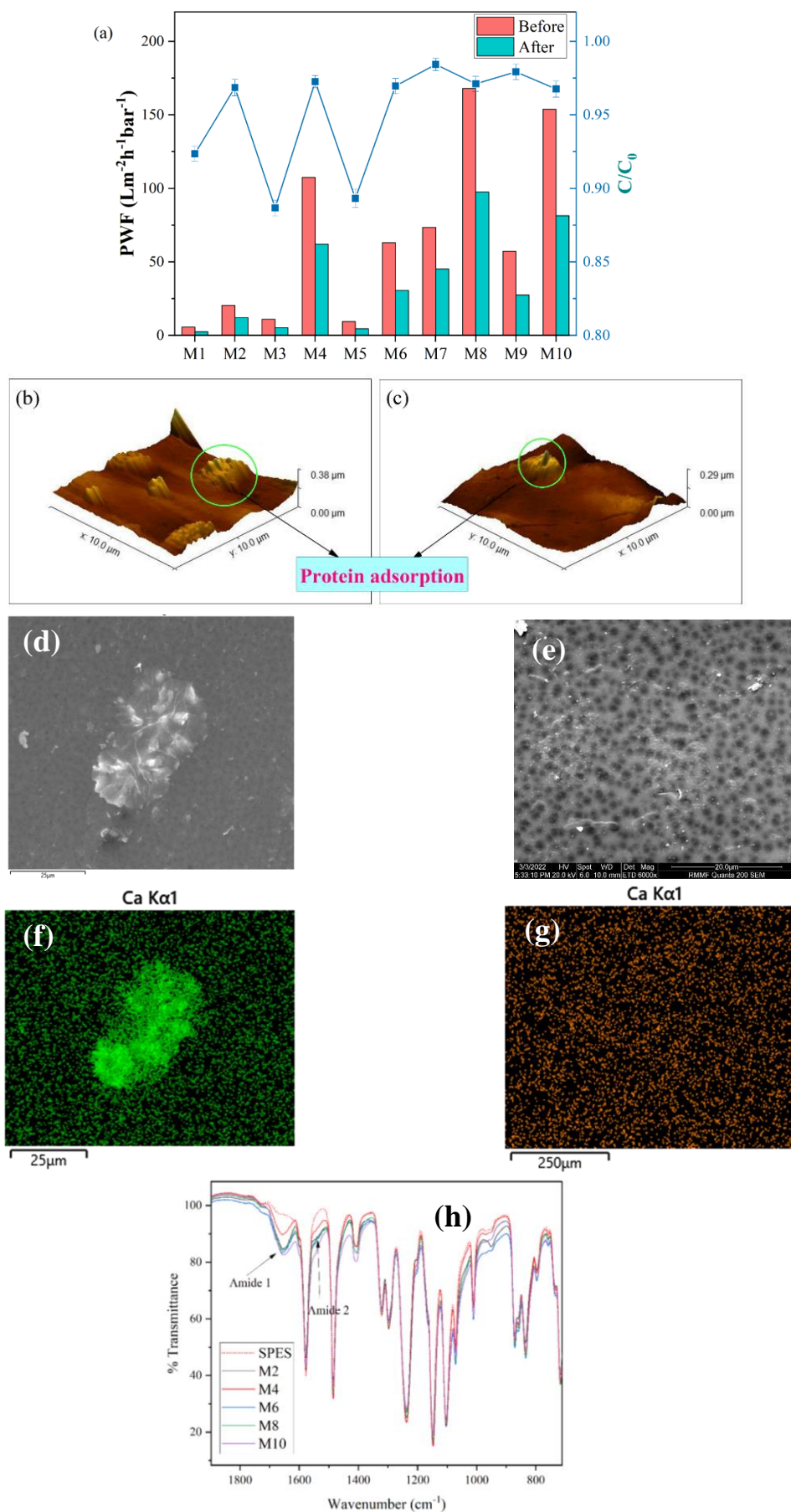
Fig. 5. (a) PWF of M1-M10 membranes before and after protein purification and relative protein concentration, AFM surface topography **(b)** neat PES **(c)** M4 after adsorption, the surface morphology of **(d)** neat PES **(e)** M4, EDS elemental analysis of Ca **(f)** neat PES **(g)** M4 **(h)** FTIR spectra of adsorbed membranes

4. Conclusion

Sulfonated polyethersulfone-based ultrafiltration membranes successfully isolated Lysozyme from the natural CEW solution, and their antifouling properties were evaluated. The morphology of the membranes was altered by controlling the demixing rate of the NIPS mechanism. The topographic and cross-section morphological changes of the PES/sPES with and without PEG (400/6000) additives and the effect of coagulation bath temperature, were investigated by AFM and SEM analysis. The surface roughness results from the AFM study revealed that the membrane fabricated from sPES has a low fouling tendency than PES. Additionally, the hydrophilicity and ion exchange capacity (IEC) on the PWF and Lysozyme separation were rationally correlated. The permeation flux of the M1-M10 membranes was enhanced when operated under cross-flow mode due to the tangential flow of the feed leading to a low concentration polarization on the membrane surface. The CEW protein permeation studies showed that the M4 membrane exhibited high permeation flux with good retention of Ovalbumin and Overtransferrin in a batch operation. The design of the semi-batch model successfully minimized feed concentration fluctuation and led to isolating the highest purity of Lysozyme under optimized conditions. The antifouling properties of the membrane are improvised with the reduced surface roughness, increased hydrophilicity, and electrostatic repulsion forces. Therefore, sulfonating PES membranes and incorporating PEG-400 offers a competent method to battle fouling in the production of Lysozyme on commercial scale.

CRedit authorship contribution statement

N. Shiva Prasad: Conceptualization, Methodology, Investigation, Formal analysis, Visualization, Roles/Writing-Original Draft.
T Aarti: Formal analysis, Visualization, Roles/Writing-Original Draft,
S. Sridhar: Supervision, Resources, Funding acquisition, Writing-Review & editing.
N.R. Choudhury: Supervision, Validation, Writing-review & editing.
S.K. Bhargava: Supervision.

Conflict of Interest Statement

The authors declare that they have no known competing financial interests or personal relationships that could have appeared to influence the work reported in this paper.

Funding

Acknowledgment

References

[1] C.-C. Lai, T.-P. Shih, W.-C. Ko, H.-J. Tang, and P.-R. Hsueh, "Severe acute respiratory syndrome coronavirus 2 (SARS-CoV-2) and coronavirus disease-2019 (COVID-19): The epidemic and the challenges," International Journal of Antimicrobial Agents, vol. 55, no. 3, p. 105924, 2020/03/01/ 2020, https://doi.org/10.1016/j.ijantimicag.2020.105924.

[2] J. A. Ferreira et al., "Protein glycosylation in gastric and colorectal cancers: Toward cancer detection and targeted therapeutics," Cancer Letters, vol. 387, pp. 32-45, 2017/02/28/ 2017, https://doi.org/10.1016/j.canlet.2016.01.044.

[3] N. Golac-Guzina et al., "Comparative Study of the Efficacy of the Lysozyme, Benzydamine, and Chlorhexidine Oral Spray in the Treatment of Acute Tonsillopharyngitis - Results of a Pilot Study," (in eng), Acta Med Acad, vol. 48, no. 2, pp. 140-146, Aug 2019, https://doi.org/10.5644/ama2006-124.252

[4] N. Amaly, A. Y. El-Moghazy, and G. Sun, "Fabrication of polydopamine-based NIR-light responsive imprinted nanofibrous membrane for effective lysozyme extraction and controlled release from chicken egg white," Food Chemistry, vol. 357, p. 129613, 2021/09/30/ 2021, https://doi.org/10.1016/j.foodchem.2021.129613.

[5] Y.-K. Chang, H.-I. Cheng, C. W. Ooi, C. P. Song, and B.-L. Liu, "Adsorption and purification performance of lysozyme from chicken egg white using ion exchange nanofiber membrane modified by ethylene diamine and bromoacetic acid," Food Chemistry, vol. 358, p. 129914, 2021/10/01/ 2021, https://doi.org/10.1016/j.foodchem.2021.129914.

[6] M. Feins and K. K. Sirkar, "Highly selective membranes in protein ultrafiltration," Biotechnology and Bioengineering, https://doi.org/10.1002/bit.20069 vol. 86, no. 6, pp. 603-611, 2004/06/20 2004, https://doi.org/10.1002/bit.20069.

[7] P. Meleady, "Two-Dimensional Gel Electrophoresis and 2D-DIGE," in Difference Gel Electrophoresis: Methods and Protocols, K. Ohlendieck Ed. New York, NY: Springer New York, 2018, pp. 3-14.

[8] J. V. Jorrin-Novo, S. Komatsu, R. Sanchez-Lucas, and L. E. Rodríguez de Francisco, "Gel electrophoresis-based plant proteomics: Past, present, and future. Happy 10th-anniversary Journal of Proteomics!," Journal of Proteomics, vol. 198, pp. 1-10, 2019/04/30/ 2019, https://doi.org/10.1016/j.jprot.2018.08.016.

[9] T. M. Przybycien, N. S. Pujar, and L. M. Steele, "Alternative bioseparation operations: life beyond packed-bed chromatography," Current Opinion in Biotechnology, vol. 15, no. 5, pp. 469-478, 2004/10/01/ 2004, https://doi.org/10.1016/j.copbio.2004.08.008.

[10] S. Großhans, G. Wang, C. Fischer, and J. Hubbuch, "An integrated precipitation and ion-exchange chromatography process for antibody manufacturing: Process development strategy and continuous chromatography exploration," Journal of Chromatography A, vol. 1533, pp. 66-76, 2018/01/19/ 2018, https://doi.org/10.1016/j.chroma.2017.12.013.

[11] K.-H. Chen, S. S. S. Wang, P.-L. Show, S.-L. Hsu, and Y.-K. Chang, "Rapid and efficient recovery of C-phycocyanin from highly turbid Spirulina platensis algae using stirred fluidized bed ion exchange chromatography," Sep. Purif. Technol., vol. 209, pp. 636-645, 2019/01/31/ 2019, https://doi.org/10.1016/j.seppur.2018.08.057.

[12] V. Halan, S. Maity, R. Bhambure, and A. S. Rathore, "Multimodal Chromatography for Purification of Biotherapeutics - A Review," Current Protein and Peptide Science, vol. 20, no. 1, pp. 4-13, // 2019, https://doi.org/10.2174/1389203718666171020103559.

[13] R. Dembczyński and W. Białas, "Pilot-scale separation of lysozyme from hen egg white by integrating aqueous two-phase partitioning and membrane separation processes," Process Biochemistry, vol. 48, no. 12, pp. 1992-1998, 2013/12/01/ 2013, https://doi.org/10.1016/j.procbio.2013.09.003.

[14] J. Brand, E. Dachmann, M. Pichler, S. Lotz, and U. Kulozik, "A novel approach for lysozyme and ovotransferrin fractionation from egg white by radial flow membrane adsorption chromatography: Impact of product and process variables," Sep. Purif. Technol., vol. 161, pp. 44-52, 2016/03/17/ 2016, https://doi.org/10.1016/j.seppur.2016.01.032.

[15] H.-T. Chiu, J.-M. Lin, T.-H. Cheng, S.-Y. Chou, and C.-C. Huang, "Direct purification of lysozyme from chicken egg white using weak acidic polyacrylonitrile nanofiber-based membranes," Journal of Applied Polymer Science, https://doi.org/10.1002/app.36764 vol. 125, no. S2, pp. E616-E621, 2012/09/25 2012, https://doi.org/10.1002/app.36764.

[16] M. Y. Arıca and G. Bayramoğlu, "Purification of lysozyme from egg white by Reactive Blue 4 and Reactive Red 120 dye-ligands immobilised composite membranes," Process Biochemistry, vol. 40, no. 3, pp. 1433-1442, 2005/03/01/ 2005, https://doi.org/10.1016/j.procbio.2004.06.028.

[17] G. Sava, A. Benetti, V. Ceschia, and S. Pacor, "Lysozyme and cancer: role of exogenous lysozyme as anticancer agent (review)," (in eng), Anticancer Res, vol. 9, no. 3, pp. 583-91, May-Jun 1989.

[18] S. Das, S. Banerjee, and J. D. Gupta, "Experimental Evaluation of Preventive and Therapeutic Potentials of Lysozyme," Chemotherapy, vol. 38, no. 5, pp. 350-357, 1992, https://doi.org/10.1159/000239025.

[19] F. Murakami, T. Sasaki, and T. Sugahara, "Lysozyme stimulates immunoglobulin production by human-human hybridoma and human peripheral blood lymphocytes," Cytotechnology, vol. 24, no. 2, p. 177, 1997/07/01 1997, https://doi.org/10.1023%2FA%3A1007936629501.

[20] L. Yan, S. Shen, J. Yun, and K. Yao, "Isolation of Lysozyme from Chicken Egg White Using Polyacrylamide-based Cation-exchange Cryogel," Chinese Journal of Chemical Engineering, vol. 19, no. 5, pp. 876-880, 2011/10/01/ 2011, https://doi.org/10.1016/S1004-9541(11)60068-2.

[21] R. Ghosh and Z. F. Cui, "Protein purification by ultrafiltration with pre-treated membrane," J. Membr. Sci., vol. 167, no. 1, pp. 47-53, 2000/03/14/ 2000, https://doi.org/10.1016/S0376-7388(99)00275-6.

[22] A. Rasic, B. Kapo, A. Avdicevic, A. Mekic-Abazovic, S. M. Jankovic, and A. Lokvancic, "Efficacy and Safety of Lysozyme, Cetylpyridinium, and Lidocaine Fixed Combination for Treatment of Chemotherapy- and Radiotherapy-Induced Oral Mucositis: a Pilot Study," (in eng), Mater Sociomed, vol. 31, no. 3, pp. 166-171, 2019, https://doi.org/10.5455/msm.2019.31.166-171.

[23] J. Brand and U. Kulozik, "Impact of the substrate viscosity, potentially interfering proteins and further sample characteristics on the ion exchange efficiency of tangential flow membrane adsorbers," Food and Bioproducts Processing, vol. 102, pp. 90-97, 2017/03/01/ 2017, https://doi.org/10.1016/j.fbp.2016.12.007.

[24] Y.-F. Guan, S.-Y. Lai, C.-S. Lin, S.-Y. Suen, and M.-Y. Wang, "Purification of lysozyme from chicken egg white using diatom frustules," Food Chemistry, vol. 286, pp. 483-490, 2019/07/15/ 2019, https://doi.org/10.1016/j.foodchem.2019.02.023.

[25] M. G. Santos et al., "Use of magnetic Fe3O4 nanoparticles coated with bovine serum albumin for the separation of lysozyme from chicken egg white," Food Chemistry, vol. 353, p. 129442, 2021/08/15/ 2021, https://doi.org/10.1016/j.foodchem.2021.129442.

[26] B.-L. Liu, C. W. Ooi, I. S. Ng, P. L. Show, K.-J. Lin, and Y.-K. Chang, "Effective purification of lysozyme from chicken egg white by tris(hydroxymethyl)aminomethane affinity nanofiber membrane," Food Chemistry, vol. 327, p. 127038, 2020/10/15/ 2020, https://doi.org/10.1016/j.foodchem.2020.127038.

[27] N. Shamsinar and S. M. Saufi, "Adsorptive Cation Exchanger Mixed Matrix Membrane Chromatography for the Isolation of Lysozyme from Chicken Egg White," Arabian Journal for Science and Engineering, vol. 41, no. 7, pp. 2479-2485, 2016/07/01 2016, https://doi.org/10.1007/s13369-015-1939-8.

[28] P. C. G. Mól, L. A. A. Veríssimo, M. R. Eller, V. P. R. Minim, and L. A. Minim, "Development of an affinity cryogel for one-step purification of lysozyme from chicken egg white," Journal of Chromatography B, vol. 1044-1045, pp. 17-23, 2017/02/15/ 2017, https://doi.org/10.1016/j.jchromb.2013.12.032.

[29] P. L. Show, C. W. Ooi, X. J. Lee, C.-L. Yang, B.-L. Liu, and Y.-K. Chang, "Batch and dynamic adsorption of lysozyme from chicken egg white on dye-affinity nanofiber membranes modified by ethylene diamine and chitosan," International Journal of Biological Macromolecules, vol. 162, pp. 1711-1724, 2020/11/01/ 2020, https://doi.org/10.1016/j.ijbiomac.2020.08.065.

[30] R. Ghosh and Z. F. Cui, "Purification of lysozyme using ultrafiltration," Biotechnology and Bioengineering, vol. 68, no. 2, pp. 191-203, 2000, https://doi.org/10.1002/(SICI)1097-0290(20000420)68:2<191::AID-BIT8>3.0.CO;2-A.

[31] M. Kumar and M. Ulbricht, "Novel antifouling positively charged hybrid ultrafiltration membranes for protein separation based on blends of carboxylated carbon nanotubes and aminated poly(arylene ether sulfone)," J. Membr. Sci., vol. 448, pp. 62-73, 2013/12/15/ 2013, https://doi.org/10.1016/j.memsci.2013.07.055.

[32] N. H. Abd-Razak, A. Pihlajamäki, T. Virtanen, Y. M. John Chew, and M. R. Bird, "The influence of membrane charge and porosity upon fouling and cleaning during the ultrafiltration of orange juice," Food and Bioproducts Processing, vol. 126, pp. 184-194, 2021/03/01/ 2021, https://doi.org/10.1016/j.fbp.2021.01.009.

[33] A. Rahimpour, S. S. Madaeni, and Y. Mansourpanah, "The effect of anionic, non-ionic and cationic surfactants on morphology and performance of polyethersulfone ultrafiltration membranes for milk concentration," J. Membr. Sci., vol. 296, no. 1, pp. 110-121, 2007/06/15/ 2007, https://doi.org/10.1016/j.memsci.2007.03.029.

[34] R. Guan, H. Zou, D. Lu, C. Gong, and Y. Liu, "Polyethersulfone sulfonated by chlorosulfonic acid and its membrane characteristics," European Polymer Journal, vol. 41, no. 7, pp. 1554-1560, 2005/07/01/ 2005, https://doi.org/10.1016/j.eurpolymj.2005.01.018.

[35] N. S. Prasad, N. L. Gayatri, B. N. Sandhya, S. Kalyani, S. K. Bhargava, and S. Sridhar, "Hydrophilized Ultrafiltration Membranes Synthesized from Acrylic Acid Grafted Polyethersulfone for Downstream Processing of Therapeutic Insulin and Cobalamin," Applied Biochemistry and Biotechnology, 2022/03/31 2022, https://doi.org/10.1007/s12010-022-03822-x.

[36] A. Rahimpour and S. S. Madaeni, "Polyethersulfone (PES)/cellulose acetate phthalate (CAP) blend ultrafiltration membranes: Preparation, morphology, performance, and antifouling properties," J. Membr. Sci., vol. 305, no. 1, pp. 299-312, 2007/11/15/ 2007, https://doi.org/10.1016/j.memsci.2007.08.030.

[37] M. Amirilargani, M. Sadrzadeh, and T. Mohammadi, "Synthesis and characterization of polyethersulfone membranes," Journal of Polymer Research, vol. 17, no. 3, pp. 363-377, 2010/05/01 2010, https://doi.org/10.1007/s10965-009-9323-6.

[38] Y.-C. Lin, H.-H. Tseng, and D. K. Wang, "Uncovering the effects of PEG porogen molecular weight and concentration on ultrafiltration membrane properties and protein purification performance," J. Membr. Sci., vol. 618, p. 118729, 2021/01/15/ 2021, https://doi.org/10.1016/j.memsci.2020.118729.

[39] J.-K. Fang, H.-C. Chiu, J.-Y. Wu, and S.-Y. Suen, "Preparation of polysulfone-based cation-exchange membranes and their application in protein separation with a plate-and-frame module," Reactive and Functional Polymers, vol. 59, no. 2, pp. 171-183, 2004/05/01/ 2004, https://doi.org/10.1016/j.reactfunctpolym.2004.01.008.

[40] Y. Manawi, V. Kochkodan, E. Mahmoudi, D. J. Johnson, A. W. Mohammad, and M. A. Atieh, "Characterization and Separation Performance of a Novel Polyethersulfone Membrane Blended with Acacia Gum," Scientific Reports, vol. 7, no. 1, p. 15831, 2017/11/20 2017, https://doi.org/10.1038/s41598-017-14735-9.

[41] N. J. Kruger, "The Bradford Method For Protein Quantitation," in The Protein Protocols Handbook, J. M. Walker Ed. Totowa, NJ: Humana Press, 2009, pp. 17-24, https://doi.org/10.1007/978-1-59745-198-7_4.

[42] K. Noel Jacob, S. Senthil Kumar, A. Thanigaivelan, M. Tarun, and D. Mohan, "Sulfonated polyethersulfone-based membranes for metal ion removal via a hybrid process," Journal of Materials Science, vol. 49, no. 1, pp. 114-122, 2014/01/01 2014, https://doi.org/10.1007/s10853-013-7682-1.

[43] M. Irfan et al., "Dual Optimized Sulfonated Polyethersulfone and Functionalized Multiwall Carbon Tube Based Composites High Fouling Resistance Membrane for Protein Separation," Membranes, vol. 12, no. 3, p. 329, 2022. [Online]. Available: https://www.mdpi.com/2077-0375/12/3/329.

[44] J. Xu, Y. Tang, Y. Wang, B. Shan, L. Yu, and C. Gao, "Effect of coagulation bath conditions on the morphology and performance of PSf membrane blended with a capsaicin-mimic copolymer," J. Membr. Sci., vol. 455, pp. 121-130, 2014/04/01/ 2014, https://doi.org/10.1016/j.memsci.2013.12.076.

[45] M. Amirilargani, E. Saljoughi, T. Mohammadi, and M. R. Moghbeli, "Effects of coagulation bath temperature and polyvinylpyrrolidone content on flat sheet asymmetric polyethersulfone membranes," Polymer Engineering & Science, https://doi.org/10.1002/pen.21603 vol. 50, no. 5, pp. 885-893, 2010/05/01 2010, https://doi.org/10.1002/pen.21603.

[46] W. Sun, T. Chen, C. Chen, and J. Li, "A study on membrane morphology by digital image processing," J. Membr. Sci., vol. 305, no. 1, pp. 93-102, 2007/11/15/ 2007, https://doi.org/10.1016/j.memsci.2007.07.040.

[47] L. Y. Ng, A. Ahmad, and A. W. Mohammad, "Alteration of polyethersulphone membranes through UV-induced modification using various materials: A brief review," Arabian Journal of Chemistry, vol. 10, pp. S1821-S1834, 2017/05/01/ 2017, https://doi.org/10.1016/j.arabjc.2013.07.009.

[48] A. Abdel-Karim et al., "Fabrication of modified polyethersulfone membranes for wastewater treatment by submerged membrane bioreactor," Sep. Purif. Technol., vol. 175, pp. 36-46, 2017/03/24/ 2017, https://doi.org/10.1016/j.seppur.2016.10.060.

[49] A. Rahimpour, S. S. Madaeni, S. Ghorbani, A. Shockravi, and Y. Mansourpanah, "The influence of sulfonated polyethersulfone (SPES) on surface nano-morphology and performance of polyethersulfone (PES) membrane," Applied Surface Science, vol. 256, no. 6, pp. 1825-1831, 2010/01/01/ 2010, https://doi.org/10.1016/j.apsusc.2009.10.014.

[50] X. Wen et al., "Fabrication of an antifouling PES ultrafiltration membrane via blending SPSF," RSC Advances, 10.1039/D1RA06354E vol. 12, no. 3, pp. 1460-1470, 2022, https://doi.org/10.1039/D1RA06354E.

[51] T. Mohammadi and E. Saljoughi, "Effect of production conditions on morphology and permeability of asymmetric cellulose acetate membranes," Desalination, vol. 243, no. 1, pp. 1-7, 2009/07/01/ 2009, https://doi.org/10.1016/j.desal.2008.04.010.

[52] C. Klaysom, S.-H. Moon, B. P. Ladewig, G. Q. M. Lu, and L. Wang, "Preparation of porous ion-exchange membranes (IEMs) and their characterizations," J. Membr. Sci., vol. 371, no. 1, pp. 37-44, 2011/04/01/ 2011, https://doi.org/10.1016/j.memsci.2011.01.008.

[53] A. C. Awadé and T. Efstathiou, "Comparison of three liquid chromatographic methods for egg-white protein analysis," Journal of Chromatography B: Biomedical Sciences and Applications, vol. 723, no. 1, pp. 69-74, 1999/02/19/ 1999, https://doi.org/10.1016/S0378-4347(98)00538-6.

[54] L. T. Yogarathinam et al., "Performance evaluation of whey flux in dead-end and cross-flow modes via convolutional neural networks," Journal of

Environmental Management, vol. 301, p. 113872, 2022/01/01/ 2022, https://doi.org/10.1016/j.jenvman.2021.113872.

[55] A. Ambrosi, N. S. M. Cardozo, and I. C. Tessaro, "Membrane Separation Processes for the Beer Industry: a Review and State of the Art," Food and Bioprocess Technology, vol. 7, no. 4, pp. 921-936, 2014/04/01 2014, https://doi.org/10.1007/s11947-014-1275-0.

[56] A. S. Gorzalski, C. Donley, and O. Coronell, "Elemental composition of membrane foulant layers using EDS, XPS, and RBS," J. Membr. Sci., vol. 522, pp. 31-44, 2017/01/15/ 2017, https://doi.org/10.1016/j.memsci.2016.08.055.

[57] M. Rabiller-Baudry, M. Le Maux, B. Chaufer, and L. Begoin, "Characterisation of cleaned and fouled membrane by ATR—FTIR and EDX analysis coupled with SEM: application to UF of skimmed milk with a PES membrane," Desalination, vol. 146, no. 1, pp. 123-128, 2002/09/10/ 2002, https://doi.org/10.1016/S0011-9164(02)00503-9.

[58] N. Islam, H. Wang, F. Maqbool, and V. Ferro, "In Vitro Enzymatic Digestibility of Glutaraldehyde-Crosslinked Chitosan Nanoparticles in Lysozyme Solution and Their Applicability in Pulmonary Drug Delivery," Molecules, vol. 24, no. 7, p. 1271, 2019. [Online]. Available: https://www.mdpi.com/1420-3049/24/7/1271.

Supplementary Information

# Isolation of Lysozyme from Chicken Egg White by Surface Charged Membranes

N. Shiva Prasad[1,2,3], Aarti Tallam[1], Namita Roy Choudhury[3], S. Sridhar[1,2*], Suresh K Bhargava[3]

[1] *Membrane Separations Laboratory, Process Engineering and Technology Transfer Division,*
CSIR - Indian Institute of Chemical Technology, Hyderabad, India-500007.
[2]*Academy of Scientific and Innovative Research (AcSIR), Ghaziabad, Uttar Pradesh, India.*
[3] *Royal Melbourne Institute of Technology (RMIT), Melbourne, VIC 3001, Australia.*

* Corresponding author; E-mail ID: sridhar11in@yahoo.com (Dr S. Sridhar)
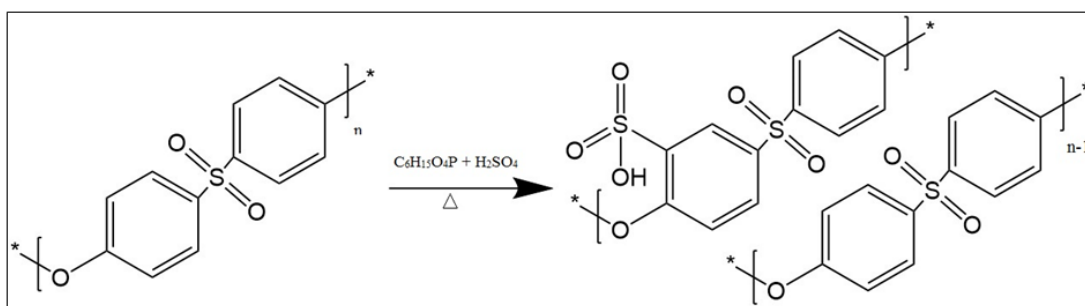
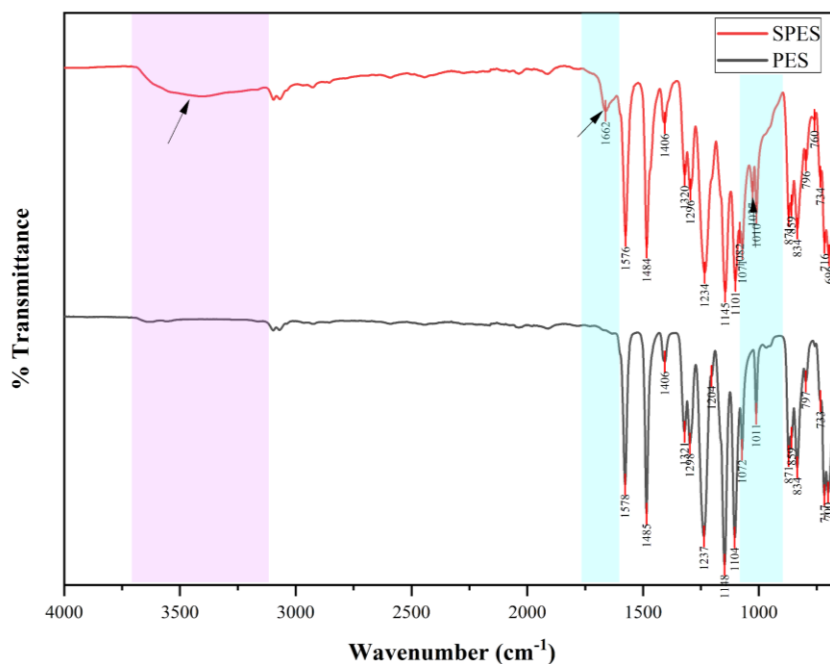**Scheme S1** Stoichiometric reaction of sulfonated polyethersulfone

Figure S1 FTIR spectra of PES and SPES

Table S1 CEW protein composition and properties

| S.NO.	CEW Protein	Composition (Abeyrathne et al., 2013)	Molecular weight (kDa)	Iso-electric point (Awadé and Efstathiou, 1999)	The net charge of protein at 7.4 pH Buffer
1	Ovalbumin	54%	45	4.6	Negative
2	Ovotransferrin	12%	76	6.1	Negative
3	Ovomucoid	11%	28	4.1	Negative
4	Lysozyme	3.50%	14.4	10.7	*Positive*
5	Ovomucin	3.50%	254	4.5	Negative
6	Avidin	0.05%	15.6	10-10.5	*Positive*
7	Cystatin	0.05%	13.3	9.3	*Positive*
8	Ovomacroglobulin	0.50%	184.7	4.5-4.7	Negative
9	Ovoflavoprotein	0.80%	32-26	4.0-4.1	Negative
10	Ovoglycoprotein	1.00%	24.4	3.9	Negative
11	Ovoinhibitor	1.50%	49	5.3	Negative
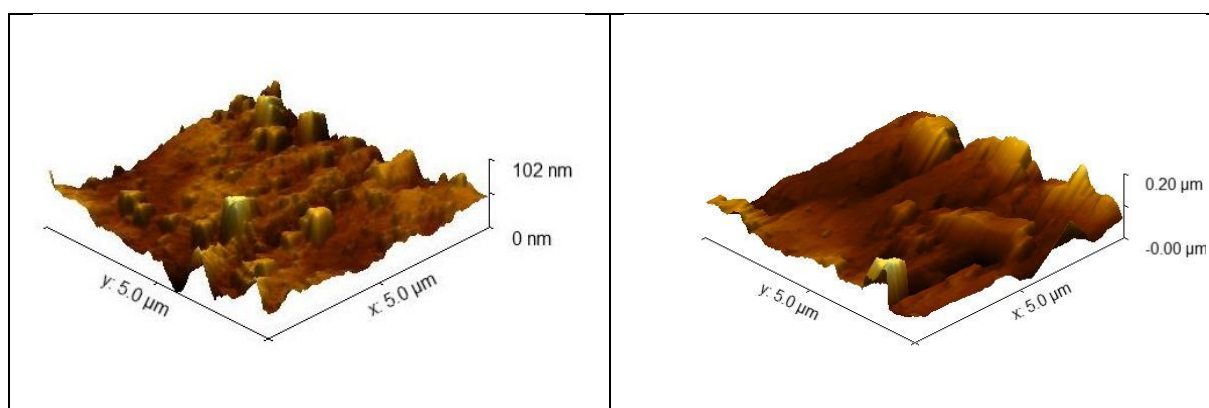
Figure S2 AFM surface topography of M4 and M8 membranes

Abeyrathne, E. D. N. S., Lee, H. Y., and Ahn, D. U. (2013). Egg white proteins and their potential use in food processing or as nutraceutical and pharmaceutical agents—A review. *Poultry Science*, *92*(12), 3292-3299. https://doi.org/https://doi.org/10.3382/ps.2013-03391

Awadé, A. C., and Efstathiou, T. (1999). Comparison of three liquid chromatographic methods for egg-white protein analysis. *Journal of Chromatography B: Biomedical Sciences and Applications*, *723*(1), 69-74. https://doi.org/https://doi.org/10.1016/S0378-4347(98)00538-6